

## Ultrasonic transit time flow meter for diesel: initial analysis

L.Svilainis, P. Kabišius, S. Kitov

*Signal processing department,  
Kaunas University of Technology,  
Studentu str. 50, LT-51368 Kaunas, Lithuania  
E-mail:linas.svilainis@ktu.lt*

### Abstract

Transport control and tracking systems allow to track the car position and other requested parameters (fuel consumption, speed, temperature etc.) over GSM networks. It is desirable to have ability to monitor the diesel fuel consumption using ultrasonic flow meter. It was suggested to use the transit time ultrasonic flow meter with beam and flow axes matched instead of conventional inclined ultrasound channel. The initial study carried out to estimate the feasibility of such device design is presented.

Numerical experiments have been carried when estimation of the time of flight was accomplished using the direct correlation method combined with parabolic sub-sample interpolation. Signal energy, operation frequency and bandwidth, electronics noise, analog to digit converter (ADC) sampling speed and resolution were taken into account.

System prototype has been designed for experimental investigation. System contains pulser, reception amplifiers, dual channel ADC with buffer memory and USB communication unit. Experiments with and without ultrasonic channel were carried out. It was concluded that under zero flow condition the transit time difference has 2,4 ps standard deviation and -0,29 ps average; virtual flow obtained has  $0.4 \cdot 10^{-4}$  m/s standard deviation and  $0.5 \cdot 10^{-5}$  m/s mean.

**Keywords:** Ultrasonic transit time flow meter, time-of-flight estimation, ultrasound electronics, fuel consumption monitoring.

### Introduction

With the rapid development of global navigation satellite systems (GNSS) and information and wireless communication technologies, the number of applications exploring the information of geographical position is expanding [1, 2]. Especially there is an increase of real time transport tracking systems [3, 4]. Started for shipping industries, tracking systems are used for solid and liquid waste collection process tracking and management, goods distribution, military and other areas. New generation of the systems is not just transmitting the position information over GSM networks in real time to the remote host but also adds vehicle speed, cabin and outdoor temperature, engine parameters, fuel consumption, remaining fuel level or even driver physiological status [5, 6]. To prevent the fuel theft by drivers it is desirable to have the ability to monitor the real time diesel fuel consumption using flow meter. The desired accuracy should be within 1 %.

Flow meters of interest can be sorted into positive displacement; inferential, oscillatory, differential pressure, ultrasonic and mass flow meters [7, 8]. The differential pressure meter possess the following advantages: the measurement is based on the accurately measurable dimensions of the primary device, no necessity for direct flow calibration, excellent reliability, reasonable performance and modest cost seems to out weight the other methods. But their high permanent pressure head loss, poor accuracy (~ 3% typically), low turndown ratio (3:1 typically) make them unsuitable for gasoline flow measurement (100:1 turndown) [7, 10]. Today the most popular meter in transport tracking systems is the positive displacement meter [9, 11]. As of inferential (mostly presented by turbine meters) it is giving a way to ultrasonic and Coriolis meters due to the need for an on-site

calibration to compensate for viscosity [7, 12]. But this type has the resistance to the flow path and consequently produces an unrecoverable pressure loss [7, 13]; also its precision is demanding clean flow, is susceptible to wear, therefore the positive displacement meters being are gradually being replaced by modern meters such as turbine, ultrasonic and Coriolis meters [7]. The Coriolis meter [14] measures mass flow directly and can provide the density also with a very high accuracy (better than  $\pm 0.1$  %). But it is subject to vibrations which is the case in vehicle on the road. Thermal mass flow meters [15] seem very attractive but due to inertness of temperature sensors and thermal propagation speeds in liquids seem complicated. So, the ultrasonic flow meter seems the best solution [16, 17]. The initial study carried out to estimate the feasibility of such device design is presented.

### Requirements

The aim is to carry the measurements in trucks, in which diesel engines are usually used. Fuel pump is taking the diesel from the fuel tank and delivers it to injection system. The injection system has its own compressor to increase the pressure in the injectors' chamber (~50 bar). The fuel pump has a higher delivery rate than it is consumed by injectors. The excess fuel is returned back to the fuel tank through a reverse valve. The valve keeps 0,7..1,4 bar pressure in order to avoid fuel gas chokes and ensure the necessary fuel amount delivery for the compressor. Such fuel circulation also ensures the cooling of pumps. The real fuel consumption is the difference between direct and return flows. Fuel consumption ranges from 3 l/h up to 120 l/h. Direct fuel flow rate is within 10...200 l/h. The diameter of the hose is 8 mm; this equals to 50 mm<sup>2</sup>. Then the mean flow velocity is 0.05...1.1 m/s.

Depending on a channel geometry, liquid properties and flow speed the flow profile is changing. To predict the type of the flow present, use is made of the Reynolds number [30, 31]:

$$Re = \frac{\rho V D_H}{\mu} = \frac{V \cdot D_H}{\nu}, \quad (1)$$

where  $\rho$  is the density of the fluid ( $\text{kg/m}^3$ ),  $V$  is the mean fluid velocity (m/s),  $D$  is the hydraulic diameter of the pipe (m),  $\nu$  is the kinematic viscosity ( $\text{m}^2/\text{s}$ ). The Reynolds number showed that the flow is laminar if  $Re$  is below 2000, transitional if  $Re=2000\dots4000$  and turbulent above 4000. At laminar flow the fully developed velocity profile is parabolic: particles move in straight lines in a laminar manner with each fluid layer flowing smoothly with no mixing between the past adjacent layers. The fluid flow profile is described as a function of the distance  $r$  from the pipe axis ratio to the pipe radius  $R$  [10]:

$$V_r = 2 \cdot V \cdot \left(1 - \frac{r^2}{R^2}\right). \quad (2)$$

At the center the speed  $V_r$  is twice the mean velocity  $V$ .

We have approached the AB „ORLEN Lietuva“ fuel properties investigation laboratory and have obtained the kinematic viscosity values at various temperatures. These values later were used to calculate the Reynolds' numbers relation to the temperature and the flow velocity range (Fig. 1).

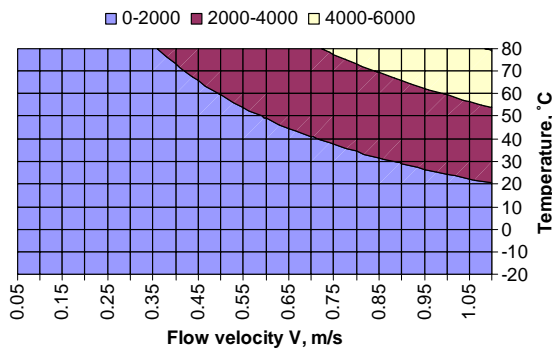


Fig.1. Reynolds' number versus flow speed and temperature

It can be concluded that at room temperatures the profile will always be laminar and only at elevated temperatures will turn into transitional. Assuming the laminar flow profile the maximum at pipe center will be 0.1...2.2 m/s. This results in 25:1 turn-down ratio (1 %).

### The ultrasonic flow meter

A few techniques can be used in ultrasonic metering: the Doppler shift [18], the pulse transit time alteration by flow [19-21], the sing-around frequency difference [22], the phase shift of two different frequencies signals [23], ultrasound propagation path properties modulation detection by two offset channels correlation [24].

We consider the ultrasonic pulse transit time technique in this study: it has been well studied, will allow for full duplex of measurement channel with least complications.

Assuming that the ultrasonic beam is matched with a flow axis, for signal to travel the distance  $L$  between ultrasonic transducers against the flow will take a longer

time  $ToF_{up}$  because the ultrasound propagation speed  $c$  will be counteracted by the flow velocity  $V$  [7, 8]:

$$ToF_{up} = \frac{L}{c - V}. \quad (3)$$

The signal travel time  $ToF_{dn}$  down the flow will be shorter because the ultrasound propagation speed will be increased by the same direction flow:

$$ToF_{dn} = \frac{L}{c + V}. \quad (4)$$

Then the flow velocity can be obtained if the distance  $L$  and the transit times  $ToF_{up}$  and  $ToF_{dn}$  are available:

$$V = \frac{L(ToF_{up} - ToF_{dn})}{2 \cdot ToF_{up} \cdot ToF_{dn}}. \quad (5)$$

Usually the transit times are combined delay of the whole system [12, 13].

At the maximum 200 l/h flow the mean velocity will be 1.1 m/s. Compared to the ultrasound velocity in diesel (1400 m/s) this is only 0.1% fraction. It was suggested to match the ultrasonic beam and flow axes instead of conventional inclined ultrasound channel (Fig. 2).

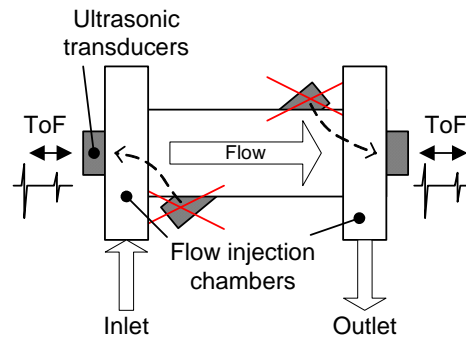


Fig.2. Suggested measuring chamber construction

In such case flow interaction with the ultrasonic beam will be maximized. This arrangement will allow to combine the direct and return flow chamber, taking the differential flow directly. The idea is not new: we have located the patent by Siemens [16] published in 1983.

Eq. 5 can be used to get the  $ToF$  influence on the  $V$  result. Sensitivity coefficients are obtained as partial derivatives:

$$\kappa_{tup} = \frac{\partial V}{\partial ToF_{up}} = \frac{L}{2 \cdot ToF_{up}^2}; \kappa_{tdn} = \frac{L}{2 \cdot ToF_{dn}^2}. \quad (6)$$

Then, assuming that both transit times  $ToF_{up}$  and  $ToF_{dn}$  are almost equal (flow velocity is only 0.1%) and have the same variability, the deviation  $\sigma_{ToF}$  in flow velocity value caused by deviation in  $ToF$  value  $\sigma_t$  can be obtained

$$\sigma_V = \kappa_{tup} \cdot \sqrt{2} \cdot \sigma_t = \sigma_t \frac{L}{\sqrt{2} \cdot ToF_{up}^2}, \quad (7)$$

or, it can be reversed for  $ToF$  accuracy requirements:

$$\sigma_t = \sigma_V \frac{\sqrt{2} \cdot ToF_{up}^2}{L}, \quad (8)$$

Again, assuming that the systematic errors can be compensated, then variability due to random  $ToF$  estimation errors is taken in further analysis. Then, for the ultrasound path length  $L$  0.1 m required  $ToF$  errors should not exceed 40 ps the for minimum flow and 800 ps for the maximum. Taking the 95% confidence interval 20 ps  $ToF$

estimation standard uncertainty for minimum flow and 400 ps for maximum are required.

### Random errors of time of flight estimation

The most important procedure in a transit time ultrasonic flow meter will be to determine the ultrasonic pulse time-of-flight ( $ToF$ ). The best case would be to find the maximum of the matched filter output. The minimal random errors produced are defined by resolution in the temporal domain

$$\delta = \frac{1}{2\pi F_e}, \quad (9)$$

where  $F_e$  is the effective bandwidth of the signal. The signal-to-noise ratio (SNR) at the matched filter output peak is given by

$$SNR = \frac{2E}{N_0}. \quad (10)$$

where  $E$  is the signal energy (Ws),  $N_0$  is the signal noise power density (W/Hz). Then minimal random errors that can be achieved by matched filter application are defined by the Cramer-Rao lower bound (CRLB) [25, 26]:

$$\sigma(ToF) \geq \frac{1}{2\pi F_e \sqrt{\frac{2E}{N_0}}}. \quad (11)$$

where  $E$  is the signal energy,  $F_e$  is the effective bandwidth of the signal. The signal  $s_T(t)$  energy can be calculated as:

$$E = \int_{-\infty}^{\infty} |s_T(t)|^2 dt = 2 \int_0^{\infty} S(f) \cdot S^*(f) df, \quad (12)$$

The effective bandwidth is given by

$$F_e^2 = \frac{\int_{-\infty}^{\infty} (f - f_0)^2 |S(f)|^2 df}{E} + \frac{\left[ \int_{-\infty}^{\infty} f |S(f)|^2 df \right]^2}{E^2}. \quad (13)$$

Eq. 11 can be reversed in order to evaluate whether such random errors as predicted by Eq. 8 are feasible by means of energy of received signal:

$$E \geq \frac{N_0}{(4\pi \cdot \sigma(ToF) \cdot F_e)^2}. \quad (14)$$

Assuming the 1 MHz effective bandwidth [28], 2 nV/ $\sqrt{\text{Hz}}$  preamplifier total input noise density [33, 34] and 10 mV received signal amplitude [32], the effective signal duration must be 1.27  $\mu\text{s}$ . Such duration can be easily achieved using non-complicated spread by phase manipulated sequence of 2-3 chips. If no spreading is assumed, with the same parameters required signal amplitude at reception should be 12mV.

Use of the digital signal involves the quantization and sampling [27]. If the sampling frequency adhered the Nyquist criteria then subsample values can be obtained using the *sinc* function. Or, at the peak position (Fig. 3) the parabolic interpolation is sufficient [29].

The peak positions  $m-1$ ,  $m$  and  $m+1$  can be used directly to find the parabolic equation for apex and  $ToF$  value is obtained directly:

$$ToF_{\#P} = \frac{1}{2} \frac{(y_{m-1} - y_{m+1})T_s}{y_{m-1} - 2y_m + y_{m+1}}. \quad (15)$$

The numerical simulation has been carried out in order to evaluate the influence of acquisition parameters on the  $ToF$  estimation performance. The signal has been simulated as CW with the Gaussian envelope and amplitude of unity.

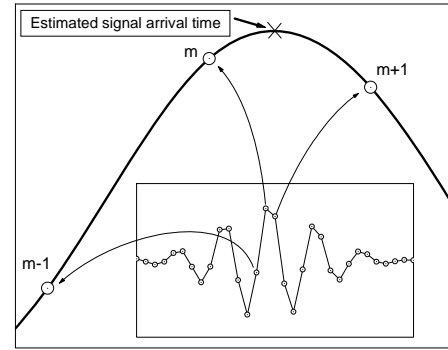


Fig. 3. Parabolic interpolation for TOF estimation

The 1 MHz center frequency and the 0.5 MHz bandwidth (-3 dB) transducer were assumed. The simulation has been carried out using MATLAB. Random errors of the  $ToF$  have been obtained by taking large number of runs (more than 1000) and obtaining the standard deviation of the  $ToF$  value estimated. The noise has been simulated using *randn* function. The SNR has been varied by changing the multiplier  $\sigma^{\#}$  of *randn* function.

In order to investigate the sampling frequency influence on the  $ToF$  estimation the sampling frequency has been varied from 1 MHz to 100 MHz (Fig.4).

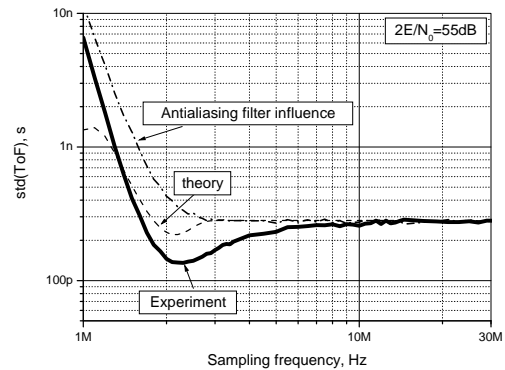


Fig. 4. The variance of TOF vs. sampling frequency

It can be seen that there is notable change in the  $ToF$  uncertainty if the sampling frequency is above 10MHz.

The carrier frequency has significant influence on the effective bandwidth [28]. This can be seen when analyzing Eq. 11 and 13: for narrowband signals the centroid of the signal spectral density  $f_0$  should prevail. The frequency  $f_0$  is actually a carrier frequency  $f_c$  of the signal. The influence of the carrier frequency on the  $ToF$  estimation performance has been investigated through numerical experiment (Fig.5).

It can be seen that the increase of the carrier frequency significantly improves the  $ToF$  estimation uncertainty. The

influence of the sampling frequency is negligible. Note the 10 times oversampling points. Such conclusion might be confusing, but it should be kept in mind that a constant noise power density was kept here and the subsample interpolation using Eq. 13 was used. The bandwidth influence is rather weak: the bandwidth close to  $f_c$  is making significant  $ToF$  errors reduction. Nevertheless, it is worth to increase the bandwidth since a larger bandwidth will allow resolution and peak detection reliability improvement.

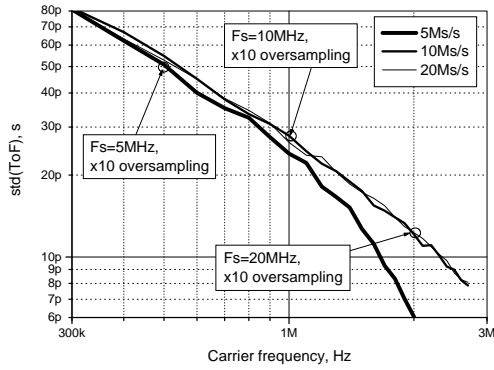


Fig. 5. Random  $ToF$  errors vs. carrier frequency

The quantization noise is related to the ADC resolution and has a direct impact on  $ToF$  variance [28]. The numerical simulation results are presented in Fig.6.

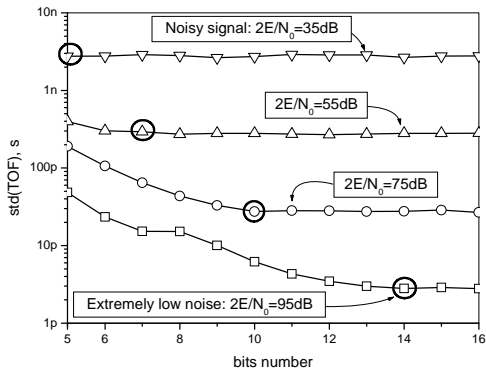


Fig. 6. Random  $ToF$  errors vs. ADC resolution

It was concluded that there is no need for the ADC resolution increase beyond the circled points: further resolution increase is swamped by electronics noise and there is no uncertainty reduction. As reference, conditions satisfying the results obtained by Eq. 14 correspond to 75 dB. It can be concluded that 10 bits then should be enough to satisfy the required uncertainty limits. The received signal strength assumed for Eq. 14 was quite pessimistic. In addition there is no need for momentary accuracy since some integration of the flow velocity will be done anyway. Besides, thanks to the matched beam and flow axes, ultrasonic beam will reside on velocity profile corresponding to the maximum speed.

### Preliminary experiments

The experimental system for transducers excitation and simultaneous up-stream and down-stream signals acquisition has been developed (Fig. 7). The system

contains pulser control logic (5 ns...2000 ns programmable duration), pulser output power stage with programmable high voltage (0 V...500 V) DC/DC regulated power supply, pulse expander, high bandwidth, high slew rate low noise amplifier with signal protection ( $\pm 0.5$  V) and filtering circuits (0.5 MHz...30 MHz Butterworth 3-rd order), dual channel programmable sampling frequency (12.5 Ms/s, 25 Ms/s, 50 Ms/s and 100 Ms/s) 10 bit flash ADC with buffer memory and glue logic, high speed USB2 interface and data host PC used for collection, storage and processing of acquired data.

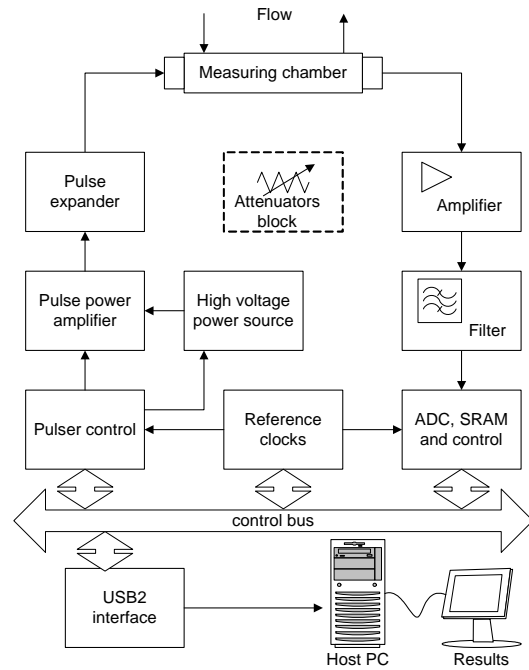


Fig. 7. Experimental system structure

In order to estimate the errors introduced by the signal acquisition electronics the dry channel (no ultrasonic transducers, no measuring chamber) experiment has been carried out. The pulser control logic output was connected to the ADC directly via 20 dB, 30 dB and 40 dB attenuator. The signals recorded were filtered using matched filter: the first signal from the record was stored as the reference and the rest used for cross correlation processing.

The sampling frequency used was 100 Ms/s and 12.5 Ms/s. Measurements were repeated 1000 times. The results of  $ToF$  estimation (parabolic subsample interpolation) were used for experiment standard deviation and mean calculation. The experiments (Fig.8) indicate, that at 20 dB attenuation the standard deviation was 5,4 ps. This is below 20 ps  $ToF$  estimation standard uncertainty required for the projected performance achievement.

Deviation from Fig.4 results here is because there was no antialiasing filter used at all. The ADC used has 300 MHz bandwidth. The noise energy from 300MHz bandwidth was distributed over 50 MHz bandwidth (first Nyquist zone) for 100 Ms/s case and over 6.25 MHz bandwidth for 12.5 Ms/s case. Therefore noise aliasing for a lower sampling rate was eight times higher.

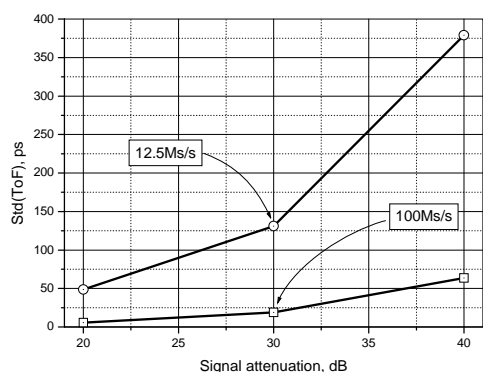


Fig. 8. Experimental standard deviation vs. signal attenuation

Another experiment was aiming to evaluate the whole electronics influence. The output of the high voltage generator was supplied directly into the amplifier’s input. The sampling frequency was 100 Ms/s, 100000 measurements were carried out at 1 Hz pulse repetition frequency. Both channels were sending the excitation signals and receiving simultaneously. The low level 10 V, excitation signal was used with duration 120 ns. The excitation generator was used for both channels, separation was through two parallel opposite connected ES1P diode pairs, and coaxial cables used had similar lengths. Fig. 9 shows the signal on ADC (red-Channel 1, blue-channel 2), Fig.10 presents the correlation function.

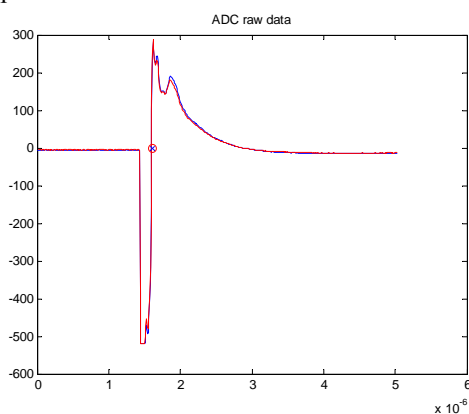


Fig. 9. Experimental signals on ADC

The signals recorded were filtered using the matched filter: the first signal from the record was stored as the reference and the rest used for cross correlation processing.

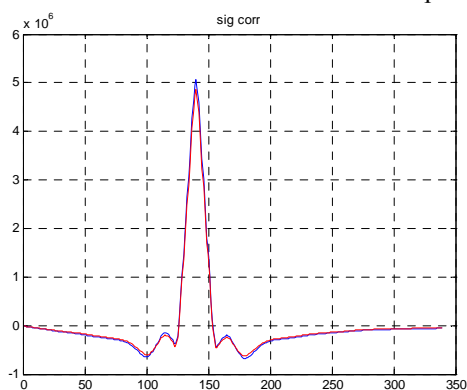


Fig. 10. Experimental signals’ correlation function

It was concluded that there is trend in the *ToF* in both channels which was attributed to the filters present in the reception channel. The obtained results for channel 1 and channel 2 *ToF* were used to calculate the difference. There was little remaining trend in *ToF* difference: the experimental standard deviation was 13 ps, mean value was -6.9 ps.

The last experiment was aiming to evaluate the ultrasonic transducers and electronics total influence. Two ultrasonic 1 MHz transducers were placed at 50 mm distance in distilled water. High voltage pulser signals were delivered to both transducers simultaneously. Separation was achieved by use of pulse expanders: two parallel opposite connected ES1P diode pairs.

There are two ways to obtain the *ToF* value: correlation is obtained between the excitation signal’s signature and the opposite channel’s propagated signal; or the same channel excitation signal signature and the propagated signal. Two techniques will differ in which delays are eliminated from the velocity calculation. After combination with Eq. 5 in the first case delays from the reception channel remain; in the second case delays of transmission channel remain. If the generator part of errors is prevailing, then it is recommended to use the first technique (opposite channels signatures). If the amplifier (reception) channel has larger errors then the second technique is preferred (same channel).

Experiments processed using the first technique (opposite channels) have showed that the experimental standard deviation was 113 ps, the mean value was -536 ps, the obtained virtual (actually it was zero) velocity of the flow was 0.0090 m/s with the standard deviation 0.0019 m/s. We would like to remind that the mean flow velocity will be changing from 0.05 m/s at 10 l/h to 1.1 m/s at 200 l/h.

Experiments processed using the second technique (same channel) indicated 2,4 ps experimental standard deviation and -0,29 ps mean value; “zero” velocity of the flow was 0.0000049 m/s with the standard deviation 0.0000049 m/s. At the pipe axis (if laminar flow) velocity is 0.1 m/s at 10 l/h. The results indicate that the ultrasonic transit time flow meter with the parameters used in initial study is feasible.

### Acknowledgment

We would like to thank Dr. A. Voleišis for support with ultrasonic transducer prototypes used in experiments.

### Conclusions

Numerical and prototype experiments were aimed to investigate whether the ultrasonic transit time flow meter for 0.05...1.1 m/s mean flow velocity at 1% expanded uncertainty is feasible. Investigation results indicate that under zero flow condition the transit time difference has 2,4 ps standard deviation and -0,29 ps average; virtual flow obtained has 0.00004 m/s standard deviation and 0.000005m/s mean. Such results make ground that ultrasonic transit time flow meter with parameters used in initial study is feasible.

## References

1. **Arebey M., Hannan M. A., Basri H., Abdullah H.** Solid waste monitoring and management using RFID, GIS and GSM. IEEE Conference on Research and Development (SCoReD). 16-18 Nov. 2009. P. 37 – 40.
2. **Toledo-Moreo R., Betaille D., Peyret F.** Lane-Level Integrity Provision for Navigation and Map Matching With GNSS, Dead Reckoning, and Enhanced Maps. IEEE Transactions on Intelligent Transportation Systems. 2010. Vol. 11(1). P. 100 – 112.
3. **Elahi M. A., Malkani Y., Fraz M.** Design and implementation of real time vehicle tracking system. Conference on Computer, Control and Communication-2009. IC4 2009. 17-18 Feb. 2009. P. 1 – 5.
4. **Humphries M., Radev P., Shirvaikar M.** A realtime vehicle tracking system. Proceedings of the Southeastern Symposium on System Theory, 2005. SSST '05. 20-22 March 2005. P.357 – 361.
5. **Rakha S. P., Farzaneh H., Zietsman M., J. Doh-Won Lee,** Development of fuel and emission models for high speed heavy duty trucks, light duty trucks, and light duty vehicles. IEEE Conference on Intelligent Transportation Systems (ITSC). 2010. P. 25 – 32.
6. **Gogate C. A., Sagaidev B. S., Vaidyanathan S. G.** Monitoring and transmission of heavy vehicle parameters using fixed cellular terminal. IEEE Vehicular Technology Conference. 26-29 Sept. 2004. P. 4100 - 4102.
7. **Crabtree M. A.** Industrial flow measurement. University of Huddersfield. June 2009.
8. **Kažys R.** Neelektrinių dydžių matavimas. Kaunas: Vitae Litera, 2007.
9. Differential fuel flow meter DPT77, JV Technoton 2010.
10. **Saleh J.** Fluid Flow Handbook. New York, NY, USA: McGraw-Hill. 2002. P. 415.
11. **Hellum A. M., Mukherjee R., Hull A. J.** Dynamics of pipes conveying fluid with non-uniform turbulent and laminar velocity profiles. Journal of fluids and structures. 2010. Vol. 26(5). P. 804-813.
12. **Pereira. M.** Flow Meters: Part 2 Part 20 in a series of tutorials in instrumentation and measurement. IEEE Instrumentation & Measurement Magazine. 2009. P.21-27.
13. Flow Control: Gas Flow Check Metering. EBSCO Industries Inc. 2010. Vol. XVI. No. 2.
14. **Röck H., Koschmieder F.** A new method to detect zero drift and sensitivity of a Coriolis Mass Flow Meter (CMFM) by using phasor control. 3rd International Conference on Sensing Technology. Taiwan 2008.
15. **Terao M.; Akutsu T.; Tanaka Y.** Non-wetted thermal micro flow sensor. SICE Conference. 2007. P. 2084 - 2088
16. **Magori V.** Ultrasonic measuring arrangement for differential flow measurement, particularly for measurement of fuel consumptions in motor vehicles with a fuel return line. US patent No 4,409,847, 1983.
17. **Eren, H.** Accuracy in real time ultrasonic applications and transit-time flow meters. IEEE Instrumentation and Measurement Technology Conference, IMTC/98. 1998. P. 568 - 572.
18. **Kenichi Tezuka, Michitsugu Mori, Takeshi Suzuki, Toshimasa Kanamine.** Ultrasonic pulse-Doppler flow meter application for hydraulic power plants. Flow Measurement and Instrumentation. 2008. Vol. 19(3-4). P. 155-162.
19. **Canqian Y., Kummel M.; Søbberg H.** A transit time flow meter for measuring milliliter per minute liquid flow. Review of Scientific Instruments. 1988. Vol. 59(2) P. 314 – 317.
20. **Som J. N.** Research and development in ultrasonic flow measurement. Journal of Pure and Applied Ultrasonics. India, July-September 2009.
21. **Raišutis R.** Investigation of a flow velocity profile in a metering section of the invasive ultrasonic flowmeter. Flow measurement and Instrumentation. 2006. Vol. 17. P.201-206.
22. **Delsing J.** The zero flow performance of a sing-around type flow meter. IEEE Ultrasonics Symposium. 1990. P. 1541 – 1544.
23. **Shan Tang Federspiel, C. C., Auslande, D.,M.** Pulsed type ultrasonic anemometer based on a double FFT procedure. IEEE Proceedings. Sensors. 2003. P. 326 – 331.
24. **Yaoying Lin, Hans V.** Self-Monitoring Ultrasonic Gas Flow Meter Based on Vortex and Correlation Method. IEEE Transactions on Instrumentation and Measurement. 2007. Vol. 56(6). P. 2420 – 2424.
25. **Rao C.** Information and the accuracy attainable in the estimation of statistical parameters. Bulletin of Calcutta Mathematics Society. 1945. Vol. 37.p. 81–89.
26. **Cramer H.** Mathematical Methods of Statistics. Princeton, NJ: Princeton Univ. Press. 1946.
27. **Kestler W. (editor).** Analog-digital conversion. Analog devices. 2004.
28. **Svilainis L., Dumbrava V.** The time-of-flight estimation accuracy versus digitization parameters. Ultragarsas 2008. Vol. 63(1). P.12-17.
29. **Svilainis L., Dumbrava V.** Analysis of the interpolation techniques for time-of-flight estimation. Ultragarsas. 2008. Vol. 63(4). P. 25-29.
30. **Zan S. J.** Experiments on circular cylinders in crossflow at Reynolds numbers up to 7 million. Journal of Wind Engineering and Industrial Aerodynamics. 2008. Vol. 96(6-7). P. 880-886.
31. **Dombrowski N., Foumeny E.A., Ookawara S., Riza A.** The influence of reynolds number on the entry length and pressure drop for laminar pipe flow. The Canadian Journal of Chemical Engineering. 1993. Vol. 71(3). P. 472–476.
32. **Zeqiri B., Gelat P. N., Barrie J., Bickley C..J.** A Novel Pyroelectric Method of Determining Ultrasonic Transducer Output Power: Device Concept, Modeling, and Preliminary Studies. IEEE Transactions on Ultrasonics, Ferroelectrics and Frequency Control. 2007. Vol. 54(11). P. 2318 – 2330.
33. **Svilainis L., Dumbrava V.** Investigation of a preamplifier noise in a pulse-echo mode. Ultragarsas. 2005. Vol. 3(56). P. 26-29.
34. **Svilainis L., Dumbrava V., Chaziachmetovas A.** Ultrasonic Preamplifier Performance Evaluation. IEEE proceedings ITI 2010. 2010. P. 663-668.

L. Svilainis, P. Kabišius, S. Kitov

#### Pradinė ultragarsinio impulsinio dyzelino srauto matuoklio analizė

#### Reziumė

Transporto kontrolės ir sekimo moduluose transporto priemonės koordinatės ir vartotojo pageidaujami išmatuoti parametrai (kuro suvartojimas, tachometro rodmenys, temperatūra ir t. t.) perduodami GSM tinklais. Pageidaujama turėti galimybę registruoti momentines kuro sąnaudas naudojant ultragarsinį dyzelino srauto matuoklį. Pasiūlytas impulsinis srauto nustatymo būdas, kai naudojamas ne įstrižas matavimo spindulys, kaip įprasta, bet ultragarso spindulys ir srautas sutapatinamas, leidžiant ultragarsą išilgai srauto. Siekiant nustatyti tokio įrenginio sukūrimo galimybes, atlikta pradinė analizė, taip pat skaitiniai eksperimentai signalo sklaidimo laiko įverčiui gauti tiesioginės koreliacijos metodu, naudojant parabolines interpoliacijos laiko patikslinimą. Įvertinta zondavimo signalo energijos, darbo dažnio, elektronikos triukšmų, skaitmeninio analogo keitiklio taktavimo dažnio ir skryos įtaka.

Eksperimentams atlikti suprojektuotas tokios sistemos prototipas. Sistemą sudaro impulsų generatorius, priėmimo stiprintuvai, dviejų kanalų 100 Ms/s skaitmeniniai analogo keitikliai su buferine atmintimi ir ryšio su USB sąsaja modulis. Atlikti eksperimentai be ultragarsinio kanalo ir su ultragarsiniu kanalu. Nustatyta, kad nesant srauto eksperimentinė standartinė deviacija skirtuminiam pralėkimo laikui yra 2,4 ps ir vidurkis yra -0,29 ps. Gautas tariamasis srauto greitis kinta esant 0,00004 m/s standartinėi deviacijai ir 0,000005 m/s vidurkiui.

Pateikta spaudai 2010-12-17